

Electronic transmission through a quantum wire by side-attached nanowires

P. A. Orellana^{a,*}, M. L. Ladrón de Guevara^a,
F. Domínguez-Adame^b

^a*Departamento de Física, Universidad Católica del Norte, Casilla 1280,
Antofagasta, Chile*

^b*GISC, Departamento de Física de Materiales, Universidad Complutense, E-28040
Madrid, Spain*

Abstract

A noninteracting system of arrays of nanowires side-coupled to a quantum wire is studied. Transport through the quantum wire is investigated by using a noninteracting Anderson tunneling Hamiltonian. An analytical expression of the conductance at zero temperature is given, showing a band with alternating forbidden and allowed minibands due to the discrete structure of the nanowires. A generalization of the odd-even parity symmetry is found in this system, whose conductance exhibits a forbidden miniband in the center of the band for an odd number of sites in the nanowires, while shows an allowed band for an even number.

Key words: Nanoscale materials, electronic transport, quantum dots
PACS: 73.21.La, 73.63.Kv, 85.35.Be

1 Introduction

Advances in nano-manufacturing have made feasible to growth nanometer sized systems, such as arrays of quantum dots [1–3], molecular wires [4] and quantum wires [5]. Quantum effects in these nanowires (NWs) are potentially useful in nanotechnology, since coupling to the continuum states shows an even-odd parity effect in the conductance when the Fermi energy is localized at the center of the energy band [6–9].

* orellana@ucn.cl

In this context, we have recently considered new quantum devices based on a NW [10] or a nanoring [11] side-coupled to a quantum wire (QW). The NW and the nanoring act as scatterers for electron transmission through the QW. These arrangements allow to tune the QW transport through the attached structure. The conductance at zero temperature through the QW shows a complex behavior as a function of the Fermi energy: far from the center of the band the conductance depends smoothly on the Fermi energy, while around the center it develops an oscillating band with resonances and antiresonances due to quantum interference in the ballistic channel.

In this work we report further progress along the lines indicated above. In particular, we study theoretically the transport properties of a set of side-coupled NWs attached to a perfect quantum wire (QW). This configuration resembles a quantum wave guide with serial side-stub structures, similar to those reported in Refs. [12–14]. We find an analytic expression for the conductance at zero temperature, which shows a band with alternating forbidden and allowed minibands. In addition, a generalization of the even-odd parity effect to the case of the Fermi energy lying at the center of the band is demonstrated.

2 Model

The system under consideration is shown in Fig. 1. The QW contains a number N of side-attached NWs with M sites of one energy level. The system, assumed in equilibrium, is modeled by a noninteracting Anderson tunneling Hamiltonian [3] that can be written as $H = H_{\text{QW}} + H_{\text{NW}} + H_{\text{QW-NW}}$, where

$$H_{\text{QW}} = v \sum_i \left(c_i^\dagger c_{i+1} + c_{i+1}^\dagger c_i \right) \quad (1a)$$

describes the dynamics of the QW, v being the hopping between neighbor sites of the QW, and c_i^\dagger (c_i) creates (annihilates) an electron in the i th site.

$$H_{\text{NW}} = \varepsilon_0 \sum_{j=1}^N \sum_{l=1}^M d_{j,l}^\dagger d_{j,l} + V_c \sum_{j=1}^N \sum_{l=1}^{M-1} (d_{j,l}^\dagger d_{j,l+1} + \text{h.c.}) \quad (1b)$$

is the Hamiltonian for the N side-attached NWs, where $d_{j,l}$ ($d_{j,l}^\dagger$) is the annihilation (creation) operator of an electron in the quantum dot l of the j th NW, ε_0 is the corresponding single level energy, and V_c the tunneling coupling between sites in the NWs, assumed all equal. The coupling of the QW with the side-attached NWs is described by the Hamiltonian

$$H_{\text{QW-NW}} = V_0 \sum_{j=1}^N \left(d_{j,1}^\dagger c_j + c_j^\dagger d_{j,1} \right), \quad (1c)$$

where V_0 is the hopping between the QW and the NWs.

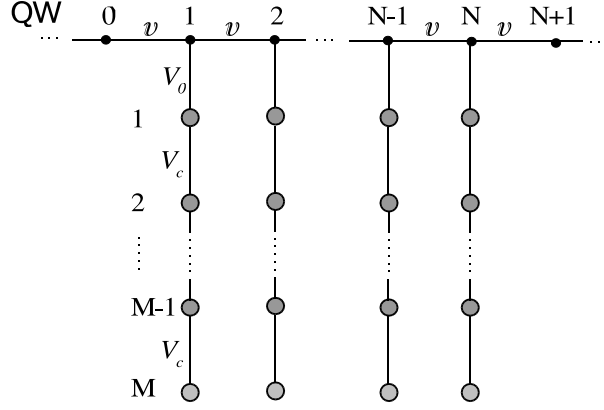


Fig. 1. N side-coupled NWs with M sites attached to a perfect QW.

The Hamiltonian for the QW, H_{QW} , corresponds to the free-particle Hamiltonian on a lattice with spacing d and whose eigenfunctions are expressed as Bloch solutions

$$|k\rangle = \sum_{j=-\infty}^{\infty} e^{ikdj} |j\rangle, \quad (2)$$

where $|k\rangle$ is the momentum eigenstate and $|j\rangle$ is a Wannier state localized at site j . The dispersion relation associated with these Bloch states reads

$$\varepsilon = 2v \cos(kd). \quad (3)$$

Consequently, the Hamiltonian supports an energy band from $-2v$ to $+2v$ and the first Brillouin zone expands the interval $[-\pi/d, \pi/d]$. The stationary states of the entire Hamiltonian H can be written as

$$|\psi_k\rangle = \sum_{j=-\infty}^{\infty} a_j^k |j\rangle + \sum_{j=1}^N \sum_{l=1}^M b_{j,l}^k |j, l\rangle, \quad (4)$$

where the coefficient a_j^k ($b_{j,l}^k$) is the probability amplitude to find the electron in the site j of the QW (l of the j th NW) in the state k , that is,

$$a_j^k = \langle j | \psi_k \rangle, \quad b_{j,l}^k = \langle j, l | \psi_k \rangle. \quad (5)$$

The amplitudes a_j^k and $b_{j,l}^k$ obey the following linear difference equations

$$a_j^k = v(a_{j+1}^k + a_{j-1}^k), \quad j \leq 0 \text{ and } j > N, \quad (6a)$$

$$\varepsilon a_j^k = v(a_{j+1}^k + a_{j-1}^k) + V_0 b_{j,1}^k, \quad j = 1, \dots, N, \quad (6b)$$

$$(\varepsilon - \varepsilon_0) b_{j,1}^k = V_c b_{j,2}^k + V_0 a_j^k, \quad j = 1, \dots, N, \quad (6c)$$

$$(\varepsilon - \varepsilon_0) b_{j,l}^k = V_c (b_{j,l+1}^k + b_{j,l-1}^k), \quad j = 1, \dots, N, \quad l = 2, \dots, M-1, \quad (6d)$$

$$(\varepsilon - \varepsilon_0) b_{j,M}^k = V_c b_{j,M-1}^k, \quad j = 1, \dots, N. \quad (6e)$$

Iterating backwards the equation for $b_{j,M}^k$ we can express the amplitudes $b_{j,1}^k$ ($j = 1, \dots, N$) in terms of a_j^k as a continued fraction

$$b_{j,1}^k = \frac{V_0 a_j^k}{\varepsilon - \varepsilon_0 - \frac{V_c^2}{\varepsilon - \varepsilon_0 - \dots \frac{V_c^2}{\varepsilon - \varepsilon_0 - \frac{V_c^2}{\varepsilon - \varepsilon_0}}}}. \quad (7)$$

Therefore the equation for a_j^k can be cast in the form

$$\varepsilon a_j^k = v(a_{j+1}^k + a_{j-1}^k) + V_0^2/Q_M a_j^k, \quad j = 1, \dots, N, \quad (8)$$

with Q_M the continued fraction

$$Q_M = \varepsilon - \varepsilon_0 - \frac{V_c^2}{\varepsilon - \varepsilon_0 - \dots \frac{V_c^2}{\varepsilon - \varepsilon_0 - \frac{V_c^2}{\varepsilon - \varepsilon_0}}}. \quad (9)$$

The above expression can be written in a more compact form as [15]

$$Q_M = V_c \sin[(M+1)\theta] / \sin M\theta, \quad (10)$$

where $\varepsilon - \varepsilon_0 = 2V_c \cos \theta$.

Let us define the renormalized energy $\tilde{\varepsilon} \equiv V_0^2/Q_M$. This contains all the information about each of the side-attached NWs. Thus, the problem reduces to one of a linear NW of N sites of effective energies $\tilde{\varepsilon}$. In order to study the solutions of (6a) and (8), we assume that the electrons are described by a plane wave incident from the far left with unity amplitude and a reflection amplitude r , and at the far right by a transmission amplitude t . That is,

$$a_j^k = e^{ikdj} + r e^{-ikdj}, \quad j < 1, \quad (11a)$$

$$a_j^k = t e^{ikdj}, \quad j > N. \quad (11b)$$

Inserting (11) into (6a) and (8), we get a inhomogeneous system of linear equations for t , r and a_j^k ($j = 1, \dots, N$), leading to the following expression

$$t = (2i/\Delta) \sin k, \quad (12a)$$

with Δ given by

$$\Delta = e^{ikN} (e^{-ik} \Delta_N + 2\Delta_{N-1} + e^{ik} \Delta_{N-2}), \quad (12b)$$

where Δ_N is the $N \times N$ determinant

$$\Delta_N = \begin{vmatrix} x & 1 & 0 & \dots & 0 \\ 1 & x & 1 & \dots & 0 \\ & \ddots & \ddots & \ddots & \\ 0 & \dots & 1 & x & 1 \\ 0 & \dots & 0 & 1 & x \end{vmatrix}, \quad (12c)$$

with $x = (\varepsilon - \tilde{\varepsilon})/v$. Δ_N can be written explicitly as

$$\Delta_N = \begin{cases} \frac{\sin [(N+1)q]}{\sin q}, & |(\varepsilon - \tilde{\varepsilon})/2v| \leq 1, \\ \frac{\sinh [(N+1)\kappa]}{\sinh \kappa}, & \text{otherwise.} \end{cases} \quad (12d)$$

For the sake of simplicity we have defined $\cos q = (\varepsilon - \tilde{\varepsilon})/2v$ and $\cosh \kappa = |(\varepsilon - \tilde{\varepsilon})/2v|$.

The transmission probability is given by $T = |t|^2$, and is related to the linear conductance G at the Fermi energy ε by the one-channel Landauer formula at zero temperature [16],

$$G(\varepsilon) = \frac{2e^2}{h} T(\varepsilon). \quad (13)$$

3 Results

Let us introduce the dimensionless conductance $g = G/(2e^2/h)$. If $|(\varepsilon - \tilde{\varepsilon})/2v| \leq 1$, $g(\varepsilon)$ reduces to

$$g = \frac{1}{\cos^2(Nq) + \left[\sin(Nq)(1 + \cos q \cos k)/(\sin q \sin k) \right]^2}, \quad (14a)$$

that is, g oscillates as a function of N and q . On the contrary, when $|\varepsilon - \tilde{\varepsilon}| > 2v$ we get

$$g = \frac{1}{\cosh^2(N\kappa) + \left[\sinh(N\kappa)(1 + \cosh \kappa \cos k)/(\sinh \kappa \sin k) \right]^2}. \quad (14b)$$

Thus, g vanishes exponentially when N is large, as a function of the product $N\kappa$, $g \sim e^{-2N\kappa}$.

The conductance is found to exhibit forbidden minibands (minigaps) that depend on the number of sites of the attached NWs. To illustrate this behavior, let us consider first the simplest cases with $M = 1$ and $M = 2$, that is, one and two sites in the side-attached arrays, respectively. Figure 2 shows the conductance versus ε for $M = 1$ and different values of the number of arrays N . For N sufficiently large, g vanishes within a range $[-\Gamma, \Gamma]$, with $\Gamma = V_0^2/2v$, and the system shows a minigap of width 2Γ . Figure 3 displays the conductance for $M = 2$. Now the minigaps take place around the bonding ($\varepsilon_- = -V_c$) and the antibonding ($\varepsilon_+ = V_c$) energies of the attached NWs. Moreover, an allowed miniband develops around the center of the band.

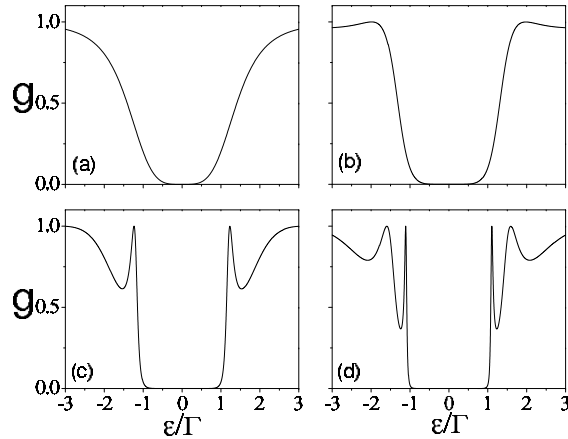


Fig. 2. Dimensionless conductance versus Fermi energy, in units of $\Gamma = V_0^2/2v$, for $M = 1$ and a) $N = 2$, b) $N = 3$, c) $N = 5$ and d) $N = 7$ when $\varepsilon_0 = 0$.

For larger M and fixed N , the system develops a set of alternating forbidden and allowed minibands in the range $[-V_c, V_c]$. Figure 4 shows the behavior of the conductance for different values of M . The number of forbidden minibands matches exactly the number of sites in the attached NWs, M , and the number of the allowed bands equals $M - 1$. Furthermore, the minigaps open around the energies in the spectrum of the isolated NW. In fact, from Eq. (14b) we can conclude that the conductance vanishes when $\kappa \rightarrow \infty$, i.e., $|(\varepsilon - \tilde{\varepsilon})/2v| \rightarrow \infty$. From Eq. (10), this condition is satisfied if $\theta = m\pi/M$ with $m = 1, \dots, M$ and the respective energies are $\varepsilon = \varepsilon_0 + 2V_c \cos[m\pi/(M + 1)]$. These energies correspond to the spectrum of an isolated NW. On the other hand, it follows from Eq. (14a) that, within each allowed miniband, the condition of maximum transmission is reached when $\sin(Nq) = 0$, i.e., $q = n\pi/N$ with $n = 1 \dots N$. Then, each allowed miniband of the conductance has N maxima. Additionally, an interesting property arises in relation to the single attached NW, namely the odd-even parity effect [10]. If the number M is odd, a forbidden band develops around center of the band while an allowed one arise for M even.

As we mentioned in the introduction, the configuration studied in this work resembles the serial side-stub structures, similar to those previously studied

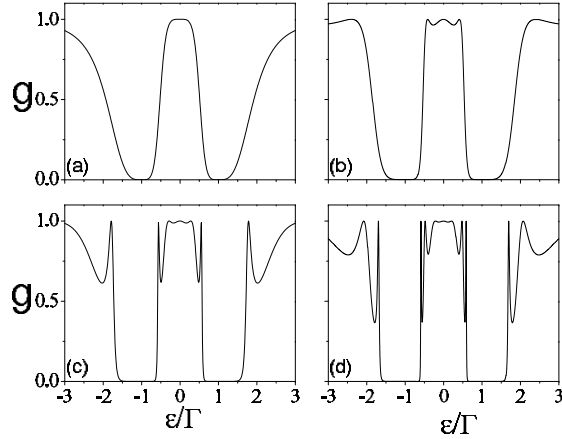


Fig. 3. Dimensionless conductance versus Fermi energy, in units of Γ , for $M = 2$, a) $N = 1$, b) $N = 3$, c) $N = 5$, and d) $N = 7$ NWs, with $V_c = \Gamma$ and $\varepsilon_0 = 0$.

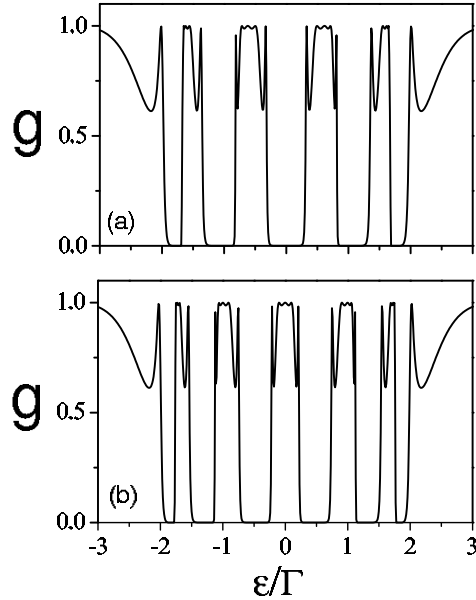


Fig. 4. Dimensionless conductance versus Fermi energy, in units of Γ , for $N = 5$ NWs, a) $M = 5$ and b) $M = 6$, sites in the NWs, with $V_c = \Gamma$ and $\varepsilon_0 = 0$.

in Refs. [12–14]. In fact, such continuous systems can also be described by our discrete model by taking $V_0 = V_c = v$ and considering the conductance around the center of the band. Figure 5 displays the conductance for a large number of attached NWs for a fixed number of attached NWs $N = 5$ ($M = 100$ and 101). Remarkably these results are similar to those obtained using continuous models. Thus, our model Hamiltonian retains the main features of the serial side-stub structures.

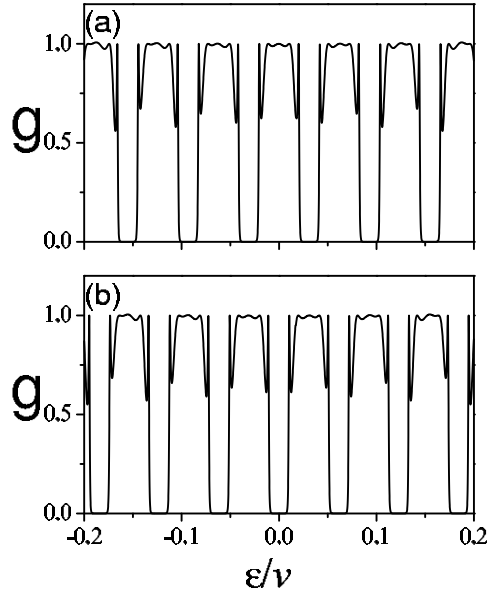


Fig. 5. Dimensionless conductance versus Fermi energy, in units of v , near the center of the bands for $N = 5$ NWs, a) $M = 100$ and b) $M = 101$ sites in the NWs, with $V_c = V_0 = v$ and $\varepsilon_0 = 0$.

4 Summary

In this work we studied the conductance at zero temperature through a QW with a set of arrays of side-attached NWs. We found that this displays an oscillating pattern with forbidden and allowed minibands, due to constructive and destructive interference in the ballistic channel, respectively. For uniform NW arrays of M sites, M minigaps and $M - 1$ allowed minibands arise. The minigaps develop around the electronic level of an isolate NW. It should be stressed that the particular setup we suggested allows us to control the energy and the width of the minibands in an independent fashion. Moreover, the system shows an odd-even parity behavior of the conductance when the Fermi energy lies at the center of the band. If the number of sites in the NWs is even, an allowed miniband is developed. On the contrary, a minigap is formed when this number is odd. This property arises from the intrinsic electronic properties of the NWs.

P. A. O. would like to thank financial support from Milenio ICM P02-054-F and FONDECYT under grants Nos. 1020269 and 7020269. M.L.L. thanks financial support from DGIP-UCN and FONDECYT grant No. 1040385. Work at Madrid was supported by DGIMCyT (MAT2003-01533).

References

- [1] A. W. Holleitner, C. R. Decker, H. Qin, K. Eberl, and R. H. Blick, *Phys. Rev. Lett.* **87**, 256802 (2001).
- [2] A. W. Holleitner, R. H. Blick, A. K. Huttel, K. Eber, and J. P. Kotthaus, *Science* **297**, 70 (2002).
- [3] W. Z. Shangguan, T. C. Au Yeung, Y. B. Yu, and C. H. Kam, *Phys. Rev. B* **63**, 235323 (2001).
- [4] A.I. Yanson, G. Rubio-Bollinger, H. E. van den Brom, N. Agrait, and J.M. van Ruitenbeek, *Nature (London)* **395**, 780 (1998).
- [5] A.T. Tilke, F.C. Simmel, H. Lorenz, R.H. Blick, and J.P. Kotthaus, *Phys. Rev. B.* **68** 075311 (2003).
- [6] R.H.M. Smit, C. Untiedt, G. Rubio-Bollinger, R.C. Segers, and J.M. van Ruitenbeek, *Phys. Rev. Lett.* **91**, 076805 (2003).
- [7] Akira Oguri, *Phys. Rev. B* **63** 115305 (2001).
- [8] Z. Y. Zeng and F. Claro, *Phys. Rev. B* **65**, 193405 (2002).
- [9] Tae-Suk Kim and S. Hershfield, *Phys. Rev. B* **65**, 214526 (2002).
- [10] P. A. Orellana, F. Domínguez-Adame, I. Gómez, and M. L. Ladrón de Guevara, *Phys. Rev. B* **67**, 085321 (2003).
- [11] P. A. Orellana, M. L. Ladrón de Guevara, M. Pacheco, and A. Latgé, *Phys. Rev. B* **68**, 195321 (2003).
- [12] P. S. Deo and A. M. Jayannavar, *Phys. Rev. B* **50**, 11629 (1994).
- [13] B.-Y. Gu, *Phys. Rev. B* **51**, 16840 (1995).
- [14] K. Nikolić, R. Sordan, *Phys. Rev. B* **58**, 9631 (1998).
- [15] H. S. Wall, *Analytic Theory of Continued Fractions* (AMS Chelsea Publishing, New York, 1967).
- [16] S. Datta, *Electronic Transport in Mesoscopic Systems* (Cambridge University Press, Cambridge, 1997).